



Images Fusion with Probabilistic Approach

Jihed Elouni

METS Research Group-National
 Engineers School of Sfax, Tunisia,

Afef Benjemmaa

METS Research Group-National
 Engineers School of Sfax, Tunisia,

ABSTRACT

In this paper we present a method for image fusion based on a probabilistic approach. The objective is to obtain a segmented image from two images representing the same scene captured at the same moment. Image resulting could then be used to estimate finer.

Keywords: probabilistic approach, GBT, Fusion, segmentation, images

1. INTRODUCTION

A technique of image fusion is based on four stages [1], namely, modeling, estimation, and combination decision. These steps are outlined below [2]:

Modeling: This stage involves the choice of a formality, and expressions of information to be merged into this formalism. The form of $(M_i^j(x))$ therefore depends on the chosen formalism.

Estimation: most models require phase estimation $(M_i^j(x))$ further information can assist in this estimate.

Combination: This step concerns the choice of a combination operator, consistent with the modeling formalism chosen.

Decision: this is the final stage of the merger, which allows you to pass information from sources the choice of a decision d_i .

The paper is organized as follows:

Section II describes the probabilistic approach used. Section III presents the Methodology and the results of the approach developed. Finally a comparative study is presented

2. APPROACH USED

In this study we used the generalized Bayes theorem defines as follows: Given two frames of discernment Ω and Θ . suppose that we know $m^\Omega[\theta_i]$ for any $\theta_i \subseteq \Theta$. If one knows with certainty that the condition is checked $X (X \subseteq \Omega)$, we show that one can obtain the mass function $m^\Theta[X]$ through the relation [3,4]:

$$zm^\Theta[X](A) = \prod_{\theta_i \in A} PL^\Omega[\theta_i](X) \cdot \prod_{\theta_i \in \bar{A}} (1 - PL^\Omega[\theta_i](X)).$$

Note that through this relationship can be inferred equal plausibility as follows:

$$PL^\Theta[X](A) = 1 - \prod_{\theta_i \in \bar{A}} (1 - PL^\Omega[\theta_i](X))$$

We suppose

$$PL^\Omega[A](X) = 1 - \prod_{\theta_i \in \bar{A}} (1 - PL^\Omega[\theta_i](X))$$

It follows the principle of reasonableness in the context of belief functions:

$$PL^\Theta[X](A) = PL^\Omega[A](X)$$

Thus, the likelihood function appears to be equal to the plausibility function. According to this principle, the likelihood of the event A knowing that the hypothesis is true X is equal to the probability of X given the assumption that A is true. In this approach, the frame of discernment, Θ is discrete. Once the combination of outcome probabilities, we must choose a decision criterion to decide which way to choose posterior probability. Several criteria are proposed in the literature, in the present study we choose as a criterion of the maximum likelihood pignistic [5].

To highlight the steps of melting and evaluate our method, we first used two synthetic images whose classes are precisely identified. These images are obtained from an image of four classes to which we added two different sounds (Gaussian and speckle noise).

In our case of image fusion, we used 5 images: two synthetic and three real. To highlight the steps of melting and evaluate our method, we applied two types of noises and sound the same values of different values on different synthetic images. Once obtained, these noisy images are used for melting.

The resulting images of the merger have mals placed pixels, this is why we applied for windows of different sizes: 3X3, 5X5, 7X7 and 9X9 to approximate the original image. Multifocal images used in the present work do not undergo any pretreatment.

Then, by applying the generalized Bayes law, we calculated the plausibility modeled after the histograms of two images to merge. Thus, pairs of gray levels (m_1, m_2) are assigned to one class of the resultant image whose plausibility is highest. At the end it is the decision phase, the decision criterion chosen in this work is the maximum likelihood pignistic.



Figure1. Example of real image used



Figure2. Example of synthetic image used

The following chart summarizes the different stages developed:

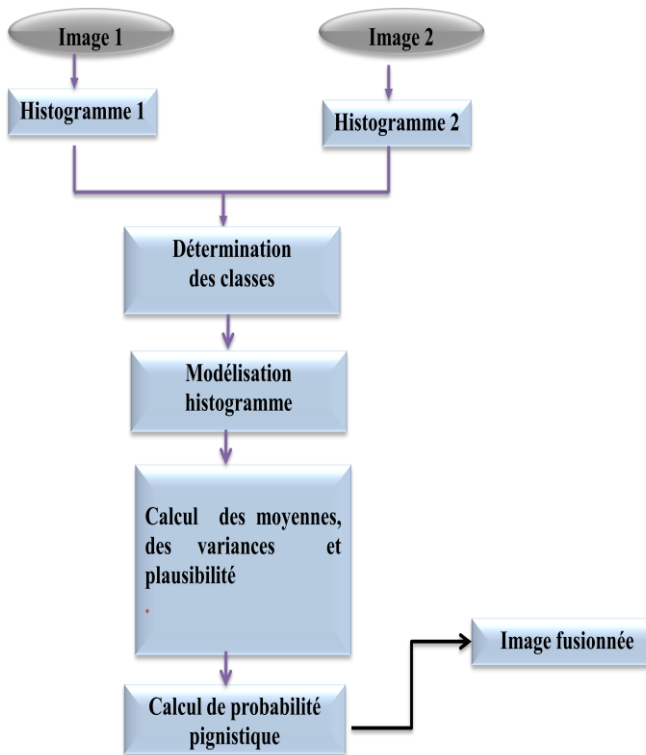


Figure3. Steps of melting

3. Methodology and Simulations results

3.1 Methodology

To develop our method, the methodology adopted in this study is as follows:

- **Test with synthetic data:** During this phase the steps performed are:
 - Generating synthetic images: during this step we determine the number of class pictures,
 - Application of two types of noise in these images: In this work we worked with speckle noise and Gaussian noise for different values of SNR,
 - Merger of these noisy images,
 - Performance evaluation of our approach by measuring the value of RMSE between the fused images and synthetic images,
 - Improved performance of fusion by applying a median filter of different sizes of window.
 - Performance evaluation of our approach by measuring the value of RMSE between the fused images after filtering and the initial synthetic images.
- **Test with real data,**
- **Comparative study:** This is to validate our approach by comparing it with a reference algorithm based on a probabilistic approach in order to evaluate the performance obtained.

3.2 Simulations results

a. types of noise used

We have applied to both synthetic images two types of noise (Gaussian and speckle) characterized by their respective means and variances. We conducted tests with different values of SNR (signal to noise ratio) described by:

$$SNR = 10 \log_{10} \frac{P_{signal}}{P_{bruit}}$$

Figure 4 shows an example of a noisy synthetic image with speckle noise of SNR = 65

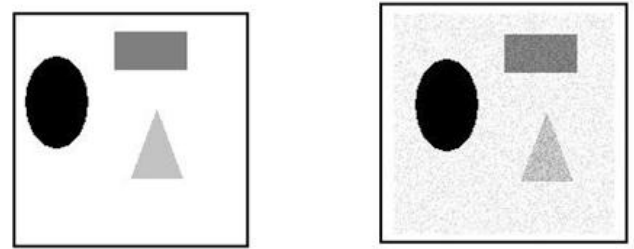


Figure4. Noisy synthetic image with speckle noise

a. Results of synthetic image

Two types of synthetic images were used:

- the first synthetic image is formed of a number of rectangles in the center of the image. Each of these rectangles is a step of the step of a given thickness. There are a total of three steps in each of the two images. With the background, so we have four objects or four classes.
- To the two synthetic image composed of three geometric shapes (rectangle, circle, triangle) the number of class is identical to frame 1.

Figure 5 shows the synthetic images used.

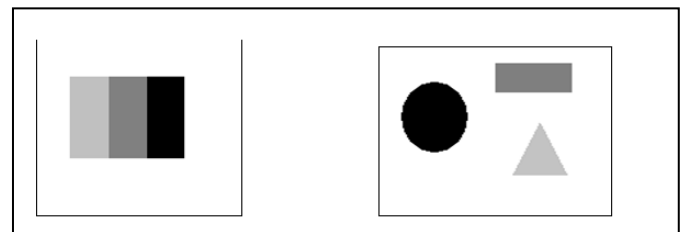


Figure5. Synthetic images used

In what follows we present some results for the two types of noise (other results found are presented in Appendix).



✚ Examples of results for a noisy image with Gaussian noise of different SNR(see figure 6 and 7)

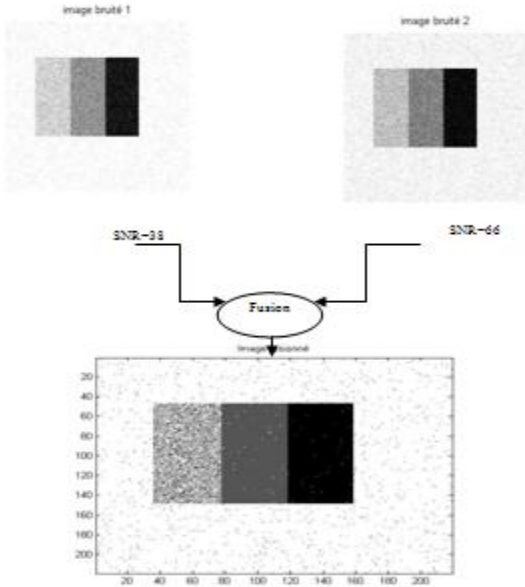


Figure6. Results for a noisy image with Gaussian noise of different SNR

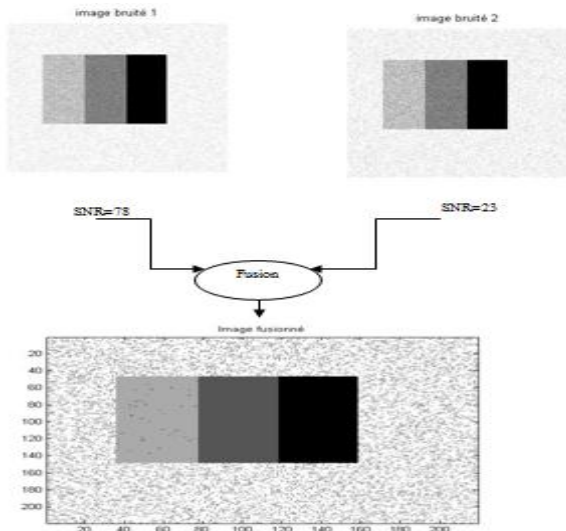


Figure7. Results for a noisy image with speckle noise of different SNR

The results found it can be concluded that the fusion results for noisy images with Gaussian noise (same values or different values) are better than those obtained by the noisy images with speckle noise. To validate our algorithm we measured RMSE (Root Mean Squared Error) between the reference images and the resulting images of fusion calculated as follows:

$$RMSE = \sqrt{\frac{\sum_{i=1}^n (x_{1,i} - x_{2,i})^2}{n}}$$

Where n is the size of images, $x_{1,i}$ the pixels of the reference image and $x_{2,i}$, the pixels of the merged image. The following tables give the values of RMSE obtained for two different fused images:

Table1. RMSE value between synthetic images and fused images using the Gaussian noise

	synthetic image1						synthetic image2							
SNR	66	38	50	30	17	33	19	85	44	68	36	53	39	54
RMSE	0,110	0,105	0,125	0,103	0,112	0,109	0,108	0,100						

Table2. RMSE value between synthetic images and fused images using the speckle noise

	synthetic image1					synthetic image2				
SNR	78	23	82	75	90	69	31	75	69	87
RMSE	0,114	0,110	0,135	0,119	0,108	0,111				

RMSE values obtained confirm that the fusion results obtained with the Gaussian noise are closer to the reference images.

After the merger, they can appear misclassified pixels, thus improving our result we have chosen to apply a median filter is particularly effective against noise in the images to grayscale. In this quit following we present some results (see figure 8 and 9):

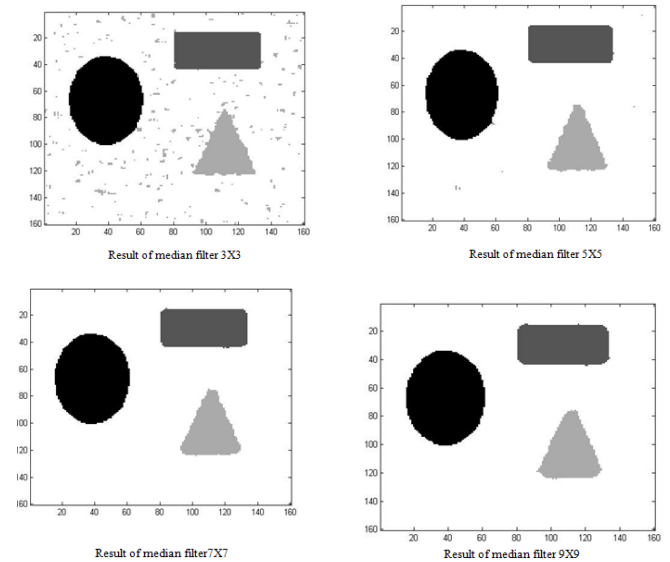


Figure8. Results of different median filter on an image resulting from the merger of two noisy images with different value of SNR

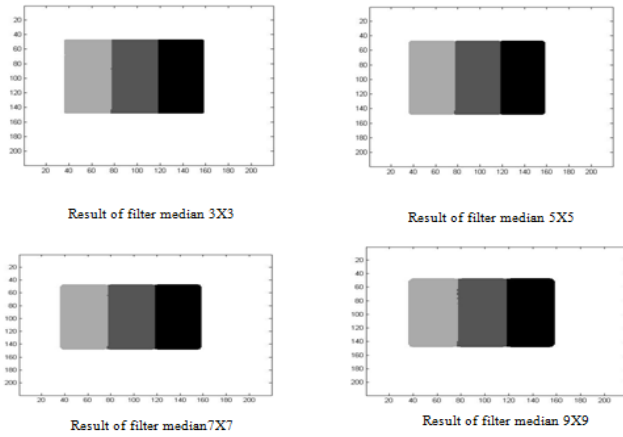


Figure9. Results of different median filter on an image resulting from the merger of two noisy images with different value of SNR

For both types of noise, we note that the larger the filter window increases, approaching the reference image. To validate our algorithm we measured the RMSE between the fused images after filtering and reference images. The following tables summarize the results.

Table3. RMSE value between the first synthetic image and filtered images (merge result using the Gaussian noise)

Median filter	SNR						
	66	38	30	17	33	19	50
3X3	0,0662		0,0242		0,0371		0,0644
5X5	0,0477		0,0452		0,0454		0,0587
7X7	0,0693		0,0607		0,0621		0,0826
9X9	0,0899		0,0771		0,0787		0,0936

Table4. RMSE value between the second synthetic image and filtered images (merge result using the Gaussian noise)

Median filter	SNR						
	85	44	54	39	53	36	68
3X3	0,7706		0,7861		0,7598		0,7737
5X5	0,7701		0,7734		0,7643		0,7715
7X7	0,7763		0,7828		0,7702		0,7755
9X9	0,7841		0,7916		0,7779		0,7827

Table5. RMSE value between the first synthetic image and filtered images (merge result using the speckle noise)

Median filter	SNR					
	78	23	75	90	82	82
3X3	0,084		0,0644		0,1109	
5X5	0,0110		0,0587		0,0657	
7X7	0,0953		0,0816		0,1046	
9X9	0,0772		0,0936		0,1441	

Table6. RMSE value between the first synthetic image and filtered images (merge result using the speckle noise)

Median filter	SNR					
	69	31	75	75	69	87
3X3	0,9347		0,7785		0,7769	
5X5	0,9416		0,7801		0,7712	
7X7	0,9451		0,7913		0,7770	
9X9	0,9520		0,8006		0,7856	

These RMSE values confirm that the results of fusion with the Gaussian noise are better than those obtained with speckle noise.

b. Results of real images

In the present work we used it multifocus three images: these images are captured for the same scene and at the same time. The melting process is as follows: from two original images with a gray area chaccone applying our method to have the merged image. The result is the following for an example of real image (see figure 10).

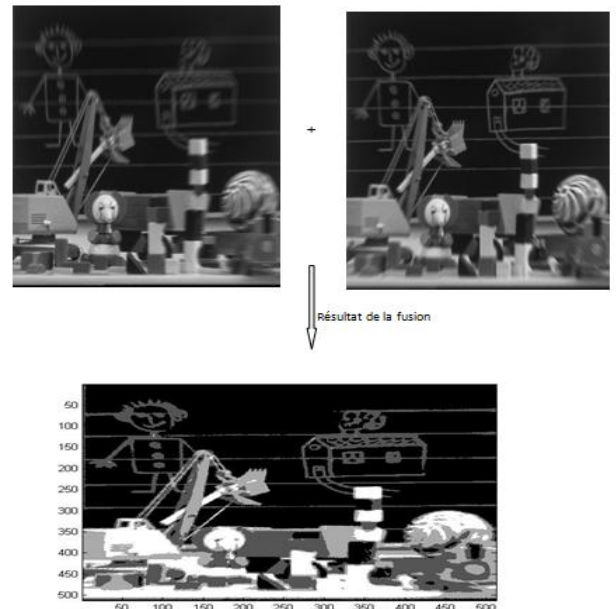


Figure10. Example of the result of fusion of a real image

4. Comparative study

By comparing the results of our probabilistic approach to image fusion developed based on Bayes' theorem generalized, with those of AMEUR.Z[6] which is also based on a probabilistic approach to image fusion but based on the law of MAP, we find that our results are better. Indeed, the RMSE



obtained for different values of SNR by our method are better than these results. In Tables 7 and 8, we summarize the results obtained by our method and that of AMEUR. Z on a synthetic image 1.

Table 7. Comparison of results of AMEUR and our results for the merged images with Gaussian noise

SNR	Our approach						AMEUR approach						
	66	38	50	30	17	33	19	66	38	50	30	17	33
RMSE	0,110	0,105	0,125	0,103	0,117	0,109	0,112	0,125					

Table 8. Comparison of results of AMEUR and our results for the merged images with speckle noise

SNR	Our approach					AMEUR approach				
	78	23	82	75	90	78	23	82	75	90
RMSE	0,114	0,110	0,135	0,119	0,118	0,151				

From these tables it can be concluded that image fusion by probabilistic approach based on Bayes' theorem is generalized outperforms the probabilistic approach based on the theorem of MAP. Indeed, the values of RMSE by our approach are better than those of AMEUR. Z

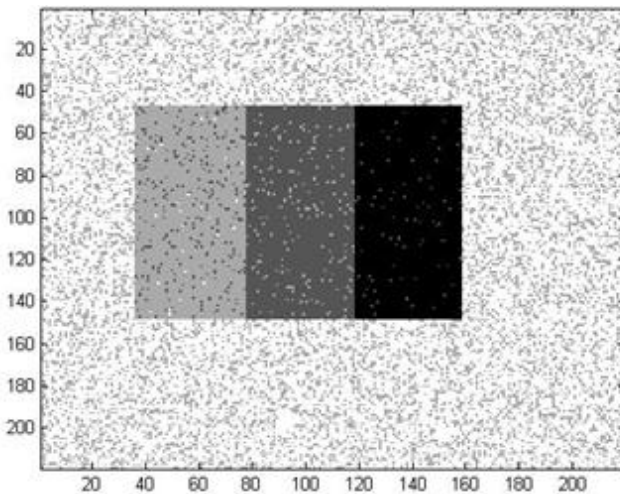


Figure 11. Result of the fusion approach AMEUR for two noisy images with Gaussian noise of different SNR

5. Conclusion

In This paper we have described the probabilistic approach used . It has been used to segment the images at the pixel level, using the gray level information as provided by the image, which makes their independent use of a particular application domain.

Probability theory is also well suited to different levels of abstraction, and solves, in a coherent theoretical framework, a complete problem detection and segmentation defects in images (defects in metal parts, medical images dan tumors). The probabilistic approach, presents a formal framework for reasoning under uncertainty, a model that allows modeling knowledge. With the introduction of masses of evidence, the attenuation coefficients of these masses and the means of the combination rule allows it processed the information developed to achieve reliability. This helps greatly in decision making, or in other areas (such as remote sensing).

6. References

- [1] LUQUE A., GOMEZ I. MANSO M. (2006). Convective rainfall rate multichannel algorithm for Meteosat-7 and radar derived calibration matrices. revue Atmosfera, Vol. 19, N°3, 145-168.
- [2] WALD L. (1999). Data fusion, Lectures notes, Ecole des mines de Paris, Centre d'Energétique groupe télédetection et modélisation.
- [3] [TAXT-94]: Taxt T., Lundervold A., Multispectral analysis of the brain using Magnetic Resonance Imaging, IEEE Transactions on Medical Imaging septembre 1994, vol. 13, No. 3, pp 470-481.
- [4] Marzouki A., Statistical segmentation of radar images, PhD Thesis, University of Science and Technology of Lille in November 1996, 156 pages.
- [5] Alain NIFLE and Roger REYNAUD An argument for the choice between maximum and decision pignistic plausibility theory of evidence, SIXTEENTH SYMPOSIUM GRETSI - 15-19 September 1997 - GRENOBLE
- [6] AMEUR Z., IDENTIFICATION OF CLOUD MASSES BY MERGER IMAGE DATA (RADAR - SATELLITE) ,Larhyss Journal, ISSN 1112-3680, n° 06, Décembre 2007, pp. 105-120 © 2007